Available online at www.sciencedirect.com

ScienceDirect

Physics Procedia 5 (2010) 125–137

Physics Procedia

www.elsevier.com/locate/procedia

LANE 2010

Influence on the dilution by laser welding of aluminum with magnetic stirring

Tang, Z.[a*]; Gatzen, M.[a]

[a]*BIAS Bremer Institut für angewandte Strahltechnik GmbH, Klagenfurter Str. 2, D-28359 Bremen, Germany*

Abstract

The Aluminum 6xxx alloys are well-known for their high susceptibility to hot cracking. It has been reported that this problem can be effectively resolved by introducing silicon into the molten pool. However, the high welding speed by laser welding process results in an inhomogeneous dilution of the silicon, which may lead to hot cracks in the Si-poor area. The idea of applying a low frequency magnetic field during laser welding process has been already carried out recently in order to make a stir effect inside the molten pool and therefore to improve the element dilution in the weld joint.

In this paper, the effects of the magnetic field on the melt flow as well as the element dilution are shown by applying copper as "tracer" inside the molten pool. Several methods were designed with different forms of copper at different positions in the workpieces to visualize the melt flow and the corresponding element dilution in different areas of the molten pool. In addition, laser welding with AlSi18 filler wire was also conducted to realize a real welding process comparing to that with "tracer". WDX analysis was then carried out to investigate how silicon distributed inside the welds with the help of magnetic stirring. The results demonstrate that a DC magnetic field, with its direction coaxial to the laser, tends to modify the melt flow dynamics at flux density up to 100mT. The results of laser welding with filler wire showed that by the help of an AC magnetic field with a frequency up to 10 Hz and flux density above 100mT, the element dilution could be improved in the weld joint. The WDX analysis showed that under the influence of an alternating magnetic field a periodicity of the silicon distribution can be achieved, which depends greatly on the magnetic frequency.

Keywords: magnetic stirring; aluminium; joining; visualisation of the melt flow; element dilution

1. Introduction

In metallurgy and metal processing applications, the magnetic field is applied to produce a magnetohydrodynamic effect to improve the melt flow leading to homogenous element distribution. Especially in casting process, a rotating

* Zhuo Tang. Tel.: +49-421-218-50-65; fax: +49 421 218-50 63.
E-mail address: tang@bias.de.

1875-3892
doi:10.1016/j.phpro.2010.08.037

or alternating magnetic field can be used to refine the grain size of the cast [1]. Another application is to remove the inclusions in the molten metal by introducing an alternating magnetic field [2].
In arc welding process, it is already a well-known technique to apply magnetic field either transverse or coaxial to the arc to realize desired influences on the arc behaviour, so that the gap bridging ability as well as the arc stability could be improved. And on the other hand, it was also observed that the magnetic fields also helped to change the weld geometry [3]. It was also investigated to apply an alternating electromagnetic field to make a "stir" effect in the molten pool aiming to improve the melt dynamics, thus to achieve a homogenous element dilution and a significant grain refinement in the weld [4][5].
In recent years the influences of electromagnetic field on laser welding process have been investigated. Kern and Huegel reported that humping could be limited to higher welding speed during CO2 laser welding with a constant magnetic field [6]. It was also found out that the weld bead shape and the geometry of the weld section could be greatly influenced by a constant magnetic field [7]. Vollertsen and Thomy suggested a new idea of introducing magnetic stirring with a low frequency field in laser welding process on the hot crack sensitive aluminum alloys [8]. It was observed that the alternating magnetic fields were capable of influencing melt flow and weld pool dilution [9].

2. Principles of the magnetic forces inside the molten pool

The theoretical approach to describe the influence of an external (constant or alternating) magnetic field on melt pool dynamics of a typical laser keyhole welding process is based on the inclusion of two associated mechanisms: First, the interaction between a magnetic field and a moving and conducting fluid with velocity field $\vec{v}_m$ will induce a current density inside the moving melt pool and base material. Second, a temporal inhomogeneous magnetic field will induce an electric field $\vec{E}_m$ into an electrically conducting media that will in turn induce eddy currents. Both current densities are described by Ohm's law:

$$\vec{j}_m = \sigma(\vec{E}_m + \vec{v}_m \times \vec{B}_{ext}) \tag{1}$$

with $\vec{j}_m$, σ and $\vec{B}_{ext}$ being induced current density, temperature depending electrical conductivity of the fluid and the external magnetic flux density, respectively. The interaction between the induced current density and the external magnetic field entails a Lorentz force inside the fluid:

$$\vec{F}_L = \vec{j}_m \times \vec{B}_{ext} \tag{2}$$

Using Maxwell's equations and Ohm's law, the required parameters to calculate the Lorentz force can be simply deduced from $\vec{B}_{ext}$ and a velocity field $\vec{v}_m$. Introducing a vector potential $\vec{A}$ and using the induction equation ($rot\vec{E} = -\dot{\vec{B}}$) together with Coulomb gauge ($div\vec{A} = 0$), the magnetic field can be described by the relation:

$$\vec{B} = \nabla \times \vec{A}. \tag{3}$$

Thus, the Lorentz force is obtained as follows:

$$\vec{F}_L = \sigma\left\{\left[\frac{\partial \vec{A}}{\partial t} \times (\nabla \times \vec{A})\right] + \left[(\vec{v}_m \times \nabla \times \vec{A}) \times \nabla \times \vec{A}\right]\right\}. \tag{4}$$

3. Experimental setup

Fig. 1a shows the working head of the experiments. It is comprised of laser optics, gas and wire tubes as well as the magnetic coil arrangement including a coil and an iron core coaxial to the laser beam, which generates a magnetic field parallel to the laser beam under the core. Fig. 1b demonstrates the work position during welding process. The welding head stays 3mm over above the work piece, where the magnetic field is well concentrated on the molten pool. The spatial distribution of the magnetic field under the iron core was measured with a hall sensor probe. As shown in Fig. 2, the zero point was set to be 3 mm under the iron core along its rotational axis, which would be also the keyhole position on the surface of the work piece during welding. As the magnetic field is rotational symmetric, the distribution of the field vectors can be described with a cylinder coordinate system. Fig. 2 depicts a cross section

of the complete cylinder system. The red rectangular marks out the area, where was estimated to be the molten pool during laser welding process.

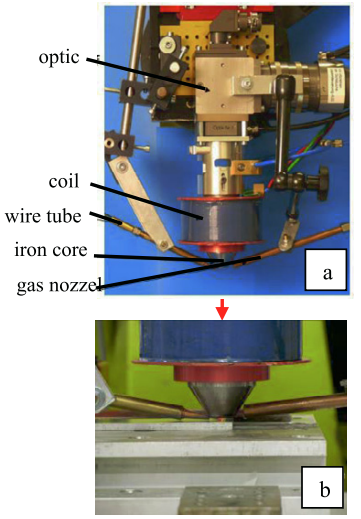

Fig. 1. Welding head combining laser optic and the Magnetic coil arrangement

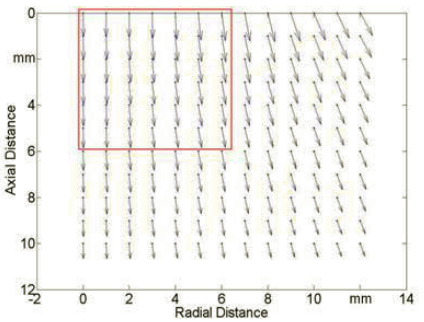

Fig. 2. Spatial distribution of magnetic flux density under the core measured with a hall sensor probe

4. Approaches to visualize and analyze the effects of magnetic stirring

In order to investigate the mechanism of magnetic stirring several Aluminum-copper model systems have been developed to demonstrate the melt flow and the element distribution inside the molten pool. Besides that, EDX and WDX was also carried out aiming to validate the results of the model systems as well as to obtain a quantitative measuring of the element dilution when welding with high silicon filler wire.

4.1. "Point" Method

The "point" method was designed to show the spatial distribution of the copper from each defined individual point. Copper wires were placed into drilled holes at depths respectively of 1mm and 3mm under the surface of a 10 mm thick aluminum plate. As shown in Fig. 3, the specimens would be welded on the side surface. When the melt pool reaches the copper, the copper wire will be melted and distribute into the molten pool with the melt flows during

welding. By the help of metallography the distribution of copper can be easily demonstrated with an optic microscope.

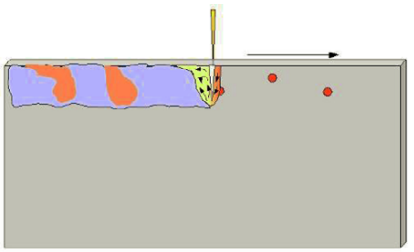

Fig. 3. Sketch of the „point“ method

(Before welding, the CuSi3 braze wires were inserted into the holes in the aluminum plate (Al 99.5), the red points on the Sketch are the Copper wires arranged transverse to the welding direction, the irregular red area denotes the distributed copper wire after welding)

4.2. “Curtain” Method

Fig.4 shows the joint configuration of the Curtain Method. The two aluminum plates will be clamped to form a butt joint, with a 0.1 mm copper foil between them. During welding the laser travels across the joint, which makes a seam perpendicular to the butt joint. Through metallography the distribution of the copper foil can be observed, which provides a clear information about how the elements from a curtain cross-section distribute inside the melt pool.

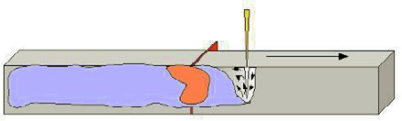

Fig. 4. Sketch of the curtain method

(Two 10 mm thick aluminum plates (Al 99.5) are clamped against each other with a copper foil (E-Cu58) between them)

4.3. Welding with copper filler wire

In order to visualize the element distribution from weld filler wire fed continuously into the melt pool, a copper wire was used instead of the normally applied Silicon contained filler wire during laser welding process, as shown in Fig.5. As it is told above, the distance between the iron core and the workpiece is only 3 mm during welding, which requires a very precise adjustment of the wire position to the laser as well as the the wire feed direction. In this investigation, both wire feed directions have been tried and it turned out that the welding process was more stable, when the wire feed direction is against the welding direction, as is shown in Fig. 5. This method makes it possible to realize a continuous copper supply into the welding pool.

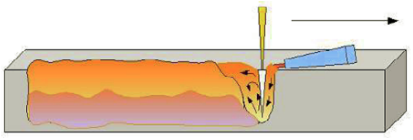

Fig. 5. Sketch of laser welding with filler wire of copper

4.4.Welding with AlSi18 filler wire

The 1.2 mm AlSi18 wire was also applied as filler wire to realize a real welding process. The wire feed position is the same as welding with copper wire as is showed in Fig. 5. 3 mm thick AA 1050 alloy was used in the experiment. All these specimens were penetrated welded.

4.5. EDX (Energy dispersive X-ray spectroscopy) and WDX (Wavelength dispersive X-ray spectroscopy)

In this study, both EDX and WDX were applied to determine the contents of the element in different parts of the weld, so that the distribution of this element can be found out. EDX line scan was used to validate the model method of welding with copper filler wire. And based on that, the dependence of element distribution on the magnetic field would be investigated. WDX mapping were carried out to get a comprehensive overview of the silicon distribution on the longitudinal sections of the welds, which were welded with high silicon contained filler wire (AlSi18). The WDX was considered to be the most directly way to investigate the silicon distribution and the effects of the magnetic stirring on the silicon dilution of the molten pool.

5. Results

5.1. "Point Method"

With the help of "point" method, the melt flow and the copper distribution can be visualized. Fig. 6 shows the longitudinal sections of the welds, which were made with different magnetic parameters. By comparing the welds, it can be seen that the copper tracer material has a bigger distribution area especially at the lower part of the weld under the influence of the alternating magnetic field. In order to describe the distribution area, the so-called distribution depth as well as the distribution length were defined, as is shown in Fig. 6. The distribution depth defines the deepest distance which the copper tracer could reach in the depth direction, while the distribution length defines the length of the copper distribution along the weld seam. Fig. 7 shows the dependence of the distribution length on the magnetic field. The copper wire, which was placed at the depth of 3 mm, tended to distribute wider along the seam after welding by increasing the magnetic frequency. In contrast, the copper wire at the depth of 1 mm tended to have a shorter distribution length at higher frequency of the alternating magnetic field. Comparing the copper distribution lengths on the same weld, the copper wire originally placed at the depth of 1mm has a longer distribution length than that of 3mm, when the magnetic frequency is below 20 Hz. Up 30Hz the copper wire at 3mm trends to distribute longer than that of 1mm along the welding direction. Fig. 6 also shows that there is no obvious correlation between the distribution depth and the magnetic field. However, this parameter only defines the maximal depth of the copper distribution. Comparing to the welds which was welded without magnetic field, more copper distributed to the lower part of the welds that were made with magnetic field.

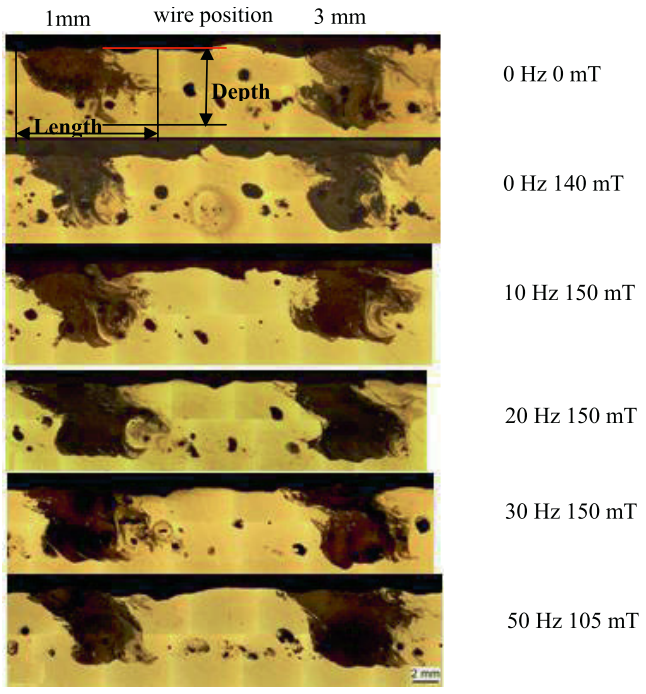

Fig. 6. Influences of the magnetic field on the melt flow by "point" method
(Longitudinal sections, weld parameter: laser power P = 6 kW; v = 6 m/min.)

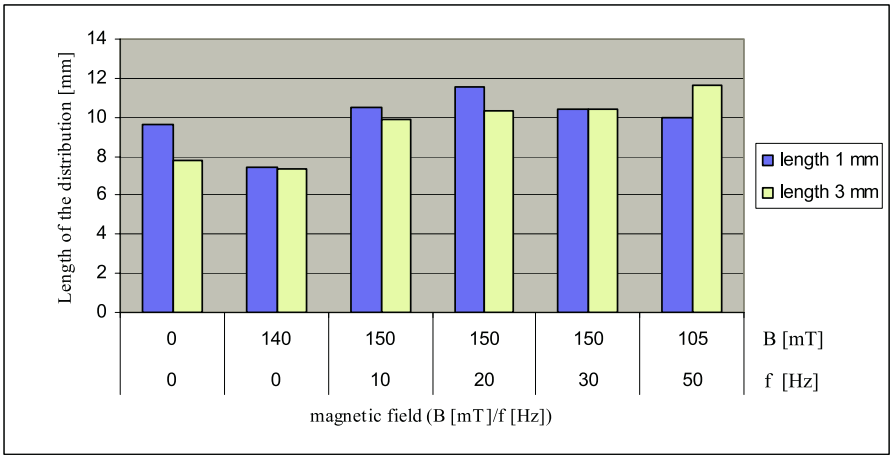

Fig. 7. Influences of the magnetic field on element distribution

5.2. "Curtain Method"

A similar phenomenon can be seen through the results of the curtain method, as is shown in Fig. 8. The only difference between "curtain" and "point" methods is the form and position of the tracer materials. The results show that the tracer tends to distribute into the lower part of the molten pool. By the magnetic flux density of 140 mT, there was an obvious convexity of the dilution in the longitudinal section, which may indicate big swirls generated by the magnetic field. Comparing the cross-sections, there was more tracer material distributing in the lower parts of the weld seams, when the magnetic flux density increases, which can also reflect the conclusions drawn though longitudinal sections of the "point" method.

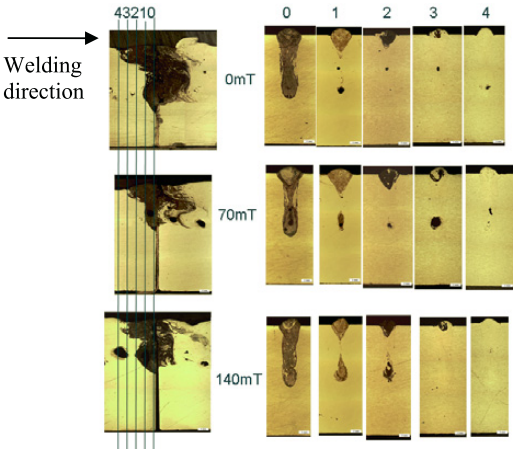

Fig. 8. Visualization of the influences of magnetic field on melt flow with curtain method (Both longitudinal (on the left part of the figure) and cross sections (on the right part of the figure) were made from the seams, which were welded with the same parameters. The numbers, 0,1,2,3,4 denote 5 different positions of cross sections, with its interval of 1mm on the seams left to the copper foil. Welding parameter: laser source: Disc laser; laser power P = 7 kW, welding speed v = 7 m/min; with AC field)

5.3. Welding with copper wire

Fig.9 shows the longitudinal sections of the welds, which were welded with different magnetic frequencies. Different color patterns can be seen on different specimens, which may indicate different element distributions. Comparing to the weld which was made without magnetic field, it appears that there are more copper distributing into the lower part of the welds. To quantify the distribution of copper, EDX line scan was carried out on the same specimens. The line scan positions and length are marked on the picture in red. The copper contents at the depth of 1mm, 3 mm and 5 mm have been investigated. At each depth, copper content in three different positions were measured and then the average value of them was defined to represent the content at this depth. The results are shown in Fig. 10. It can be seen that at the depth of 3 mm, the copper content increases with the magnetic frequency until 18 Hz. Comparing all the specimens, the most homogenous weld within the parameter envelope investigated was obtained at the magnetic field of 10 Hz. However, no obvious trend or dependence of the magnetic frequency on the element dilution has been found out in the depth of 5 mm.

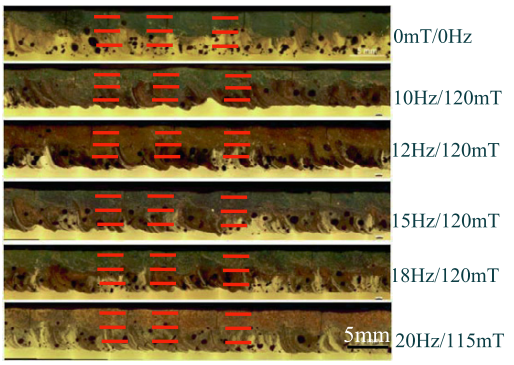

Fig. 9. Visualization of the element dilution under the influences of magnetic field (Longitudinal sections of the welds, which were made by laser welding with copper filler wire. By the help of metallography the copper-rich area shows a dark color on the micrographs; Welding parameter: Laser Power = 7 kW; welding speed=6m/min; wire feeding rate=4 m/min)

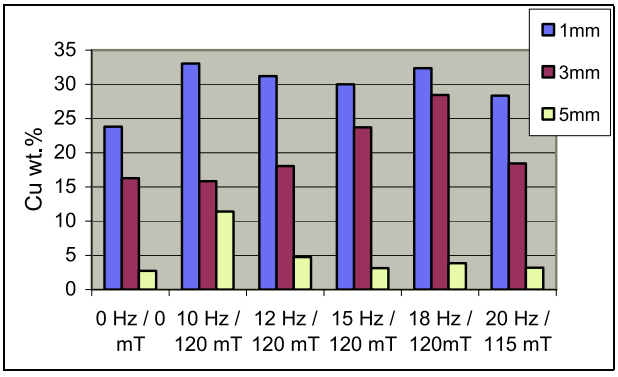

Fig. 10. Copper content at different depths in the longitudinal sections of the welds (The copper content was measured at three different depths, respectively 1 mm, 3 mm and 5 mm under the surface. At each depth on each specimen, three line scans were carried out with EDX. (The positions of the line scans are marked in Fig. 11 in red) The average of the results of these three line scans was considered to stand for the copper content at the respective depth.)

5.4 Welding with AlSi18 filler wire

Fig. 11 shows the silicon distribution on the longitudinal sections of the welds welded with AlSi18 filler wire with magnetic field. The red lines denote the areas, where a bright “tail” of the silicon can be seen in the lower part of welds. It can be indicated that under the influences of the alternating magnetic field, an approximate periodicity of the silicon distribution can be observed, especially when the magnetic frequency is up 20 Hz, comparing to the weld which was welded without magnetic field. In fig.11b there are also such silicon “tails”, but along the whole longitudinal section no periodicity can be recognized. In fig.11c, the distance between the silicon “tails” varies greatly along the weld seam, which indicates that, except the magnetic field another factor has also a strong effect on the silicon distribution. In fig.11d there are 7 cycles of the silicon distribution to be observed, while in fig. 11e with 8 obvious cycles. Fig. 12 shows the distance between the red lines at the frequency of 10 Hz, 20 Hz and 30 Hz respectively. At 10 Hz and 20 Hz the distance varies greatly comparing to the that at 30 Hz, indicating a stable periodicity of the silicon distribution at 30 Hz.

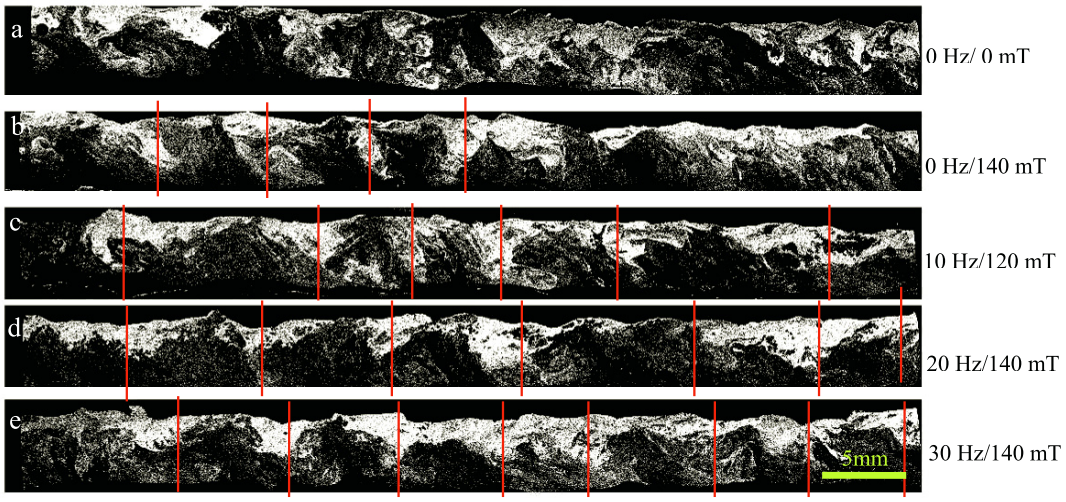

Fig. 11. WDX mappings of the longitudinal sections of welds with different magnetic fields
(Welding parameters: laser power = 5.5 kW; welding speed = 8 m/min; wire feeding speed = 6 m/min)

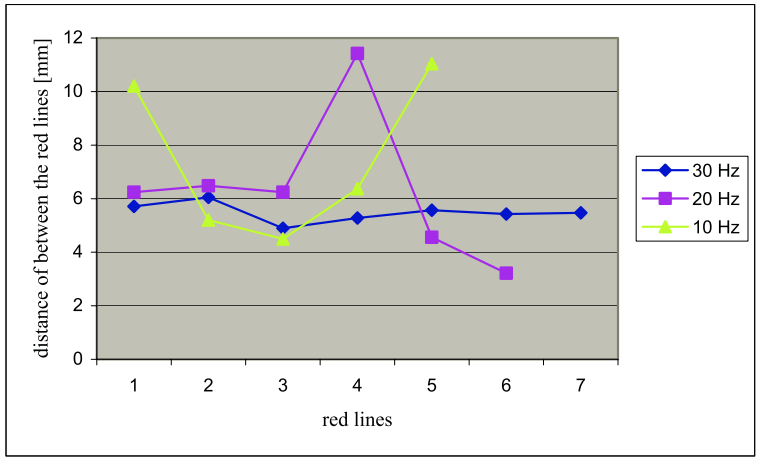

Fig. 12. The distance between the bright tails of the silicon at each frequency

Based on the results of Fig. 12, the quotient between the welding speed and the mean distance of each cycle was defined as the frequency of the silicon distribution. Fig. 13 shows the relationship between the frequency of silicon distribution and the frequency of the magnetic field. With increasing the magnetic frequency more cycles of the silicon distribution could be generated along the weld.

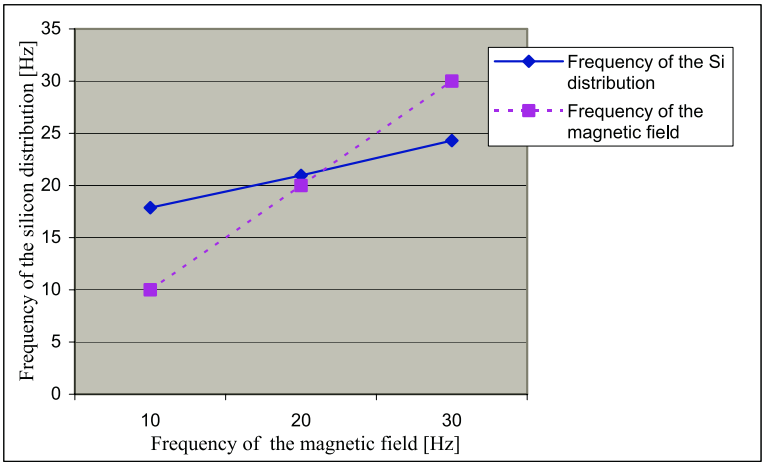

Fig. 13. Relationship between the frequency of silicon distribution and frequency of magnetic field

Fig. 14 shows the mean silicon content at different depths of the welds at different magnetic frequencies. The result shows that, a more inhomogeneous silicon distribution has been achieved in the longitudinal section of the welds with magnetic field especially at 0 Hz and 30 Hz, which is great different from the results of the welding with copper filler wire, Fig. 10.

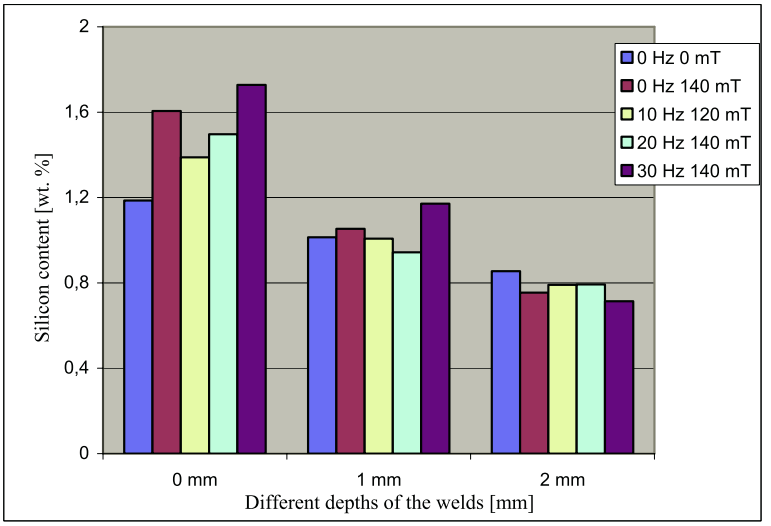

Fig. 14. The mean silicon distribution at different depth of the welds

6. Discussion

In this investigation, three model systems were set up using copper as tracer material in order to visualize the melt flow and the element dilution in the molten pool by laser welding. By means of metallography, the distribution of the copper on the weld sections can be easily and clearly distinguished, which gives a good possibility to visualize

the distribution of the tracer and reflect the melt flow. Furthermore, by comparing the specimens welded under the magnetic field, the influences of magnetic field on the melt flow and element dilution could be analyzed. The results indicate that each model system has its advantages and disadvantages in terms of visualizing the influence of magnetic field. The "point" method and the "curtain" method proved to be suitable to visualize the spatial element distribution from a single point or single cross-section in the weld seam. As fig. 7, the results of the "point" method indicate that the magnetic field helps to increase the distribution length along the welding direction, especially to increase the distribution length of the tracer materials at the lower part of the molten pool, when increasing the magnetic frequency. By means of the "curtain" method, the influence of the magnetic field, which modifies the melt flow to bring more element from the upper part down to the lower part of the weld, has been observed. With both of the two methods, a big swirl generated by the magnetic field at the lower part of the molten pool can be observed. This phenomenon can also be considered to be a clue that the magnetic field helps to modify the melt flow. As is known, the external magnetic field will generate a Lorenz force inside the molten pool, which theoretically explains how magnetic field influences the melt flow. According to the analytical model introduced by Gatzen und Tang [10], using a cylindrical coordinate (r,Φ,z system) in a rotation symmetric magnetic field (with only a non-zero component in the z-axis), the Lorenz force can be described as follows:

$$F_L = \begin{pmatrix} F_r \\ F_j \\ F_z \end{pmatrix} = -\sigma \times B_0^2 \begin{pmatrix} \omega \frac{r}{4} R(r,z) \sin(2\omega t) \\ v_j \varphi(r,z) \cos^2(\omega t) \\ \omega \frac{r}{8} Z(r,z) \sin(2\omega t) \end{pmatrix} \quad (6)$$

with F_L, σ ,B_0 being the Lorenz force in terms of volume force; temperature depending electrical conductivity of the fluid; magnitude of the magnet field, respectively; R(r,z), Φ(r,z) and Z(r,z) being distribution factors of the force components; ω as the angular frequency of the magnetic field; and v as the velocity of the fluid. It can be seen from eq. (6) that by such a low frequency magnetic field applied in this investigation, the azimuthal component of the Lorenz force FΦ plays a main role comparing to the other two components. It indicates that in this investigation, the Lorenz force inside the molten pool was proportional to the square of the magnetic flux density and the fluid velocity and always directed against the melt flow, which leaded to a brake effect (like the well-known electromagnetic brake) on the melt flow. According to Fig. 2, the magnetic flux density decreases with the axial distance, which means the Lorenz force also decreases with the axial distance. In the molten pool , there is a gradient of the Lorenz force with a downward direction. The Lorenz force itself together with its gradient, gravity as well as surface tension damp the melt flow down and bring more element into the lower part of the weld. In this way, the phenomena, which were especially observed by "curtain" and "point" methods, can then be understood. However, these two methods are limited to visualize the distribution of element from a single point or section in the weld. The model system of welding with a copper filler wire was considered to make a continuous feeding of tracer material into the molten pool, which was closer to the real welding process with normal filler wire. Through this method, the general distribution of the element originally from the filler wire inside the weld can completely be well visualized. It offered a possibility to investigate the influence of the magnetic field on the element distribution inside the entire weld. The corresponding EDX results show that the magnetic field may have an influence on the copper distribution in the middle part of the weld. However, the magnetic field seemed to be not strong enough to modify the melt flow to bring more copper into the bottom part of the welds. The WDX mapping results reveal a periodicity of the silicon distribution in the welds, which were made by alternating magnetic field. However, this periodicity is not so stable at 10 Hz and even at 20 Hz, Fig. 12. It was considered that, the length of the molten pool has interfered or limited the periodic effects of the magnetic field on the molten pool. In this project, high speed imaging has been also carried out to observe the molten pool during welding. The results showed that, the length of the molten pool on the surface is about 10mm when the welding speed at 8 m/min. As is showed in Fig. 1, the magnetic field moves with the laser beam during welding. The relationship between the molten pool length and the wavelength of magnetic field can be denoted in Fig. 15. By 10 Hz the wavelength of the magnetic field is longer than the molten pool, which means the magnetic field could not complete a whole cycle before the solidification of the molten pool. Increasing the magnetic frequency can realize more cycles of the alternating magnetic field before the molten pool solidifies. And it indicates the necessity to increase the magnetic frequency in the future work. As Fig 14, the results of the mean silicon content at different depths of the welds revealed a great different conclusion from that of

welding with copper wire. The magnetic stirring could improve the distribution of the copper element, as Fig. 10. In contrast, the most homogeneous silicon distribution has been achieved when without magnetic field at current parameter envelops. The reason of this difference may be that, in the aluminium-copper model system, the existence of copper inside the molten pool changes the viscosity. Besides, an additional Lorenz fore would be generated through the interaction of the magnetic field and thermoelectric current between copper and aluminium in the molten pool, which might influence the element dilution. But even though, the influence of the magnetic field on the melt flow as well as the element distribution were observed not only with Al-Cu model systems but also in normal welding process with AlSi18 filler wire. More detailed experiments with larger parameter envelop especially with higher magnetic frequency and flux density are needed to reveal a better understanding of the influence of the alternating magnetic field on the melt flow and the element dilution in the molten pool.

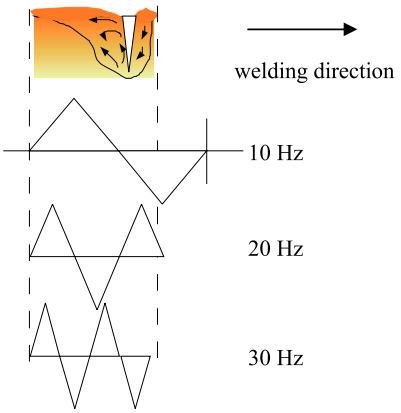

Fig. 15 The relationship between the length of molten pool and the wavelength of magnetic field during welding

7. Conclusion

In this study, the influences of the magnetic field on the melt flow and the element dilution in laser welding of aluminum were investigated. The main results are as follows:

--- “Point” and “Curtain” Methods turned out to be good methods to visualize the effect of magnetic field on the melt flow and the distribution of element from a single point or section in the weld. The experimental results help to support the hypothesis, that the magnetic field tends to make a brake effect on the melt flow and helps to improve the distribution of the tracer materials in the lower part of the molten pool .

--- The model system of welding with copper filler wire made it possible to visualize the influence of magnetic field on the distribution of the element from the filler wire.

--- The results of the WDX mapping shows that, a periodicity of the silicon distribution could be seen along the welds under the influence of the alternating magnetic field, which depends on the magnetic frequency.

Acknowledgements

The authors appreciate the funding of the Project VO530/29-1 from DFG (Deutsche Forschungsgemeinschaft) sincerely.

References

1. Asai, S., Nishio N., Muchi I.: Theo. Analysis and Model Exp. on Electromag. Driven Flow in Continuous Casting. In: Transactions of the Iron and Steel Institute of Japan Vol.22, No.2 (1982), pp.126-133.

2. J.P.Park, Y. Tanaka, K. Sassa, and S. Asai. : Elimination of tramp elements in molten metal using electromagnetic force. In Proc. 1st Int. Symp. Electromagn. Processing Master., Nagoya, Japan, ISIJ, 1994,pp. 497-504.

3. Matthes, K.-J.; Richter, E.: Schweißtechnik-Schweißen von metallischen Konstruktions-werkstoffen. München: Hanser 2002.

4. Matsuda, F.; Nakagawa, H.; Nakata, K.; Ayani, R.: Effect of electromagnetic stirring on weld solification structure of aluminium alloys (Report I). In: Trans. of JWRI, 7 (1978) 1, 111-127.

5. Matsuoka, T.; Yoshida, T.; Yamaoka, H.; Kim, C.C.: Application of magnetic stir welding to dissimilar metal structural weld overlay. In Proc. 8th International Welding Symposium. Kyoto, Japan 2008.

6. Kern, M.; Berger, P.; Hügel, H.: Magneto-Fluid-Dynamic Control of Seam Quality Seam Quality in CO2 laser beam welding. In: Welding Journal (2003) 3, 72-78.

7. Lindenau, D.; Ambrosy, G.; Berger, P. u.a.: Magnetisch beeinflusstes Laserstrahlschweißen. In: Proc. Stuttgarter Lasertage SLT' 99, Stuttgart 1999, 39-56.

8. Vollertsen, F; Thomy, C.: Magnetic Stirring during Laser welding of Aluminium. In: Journal of Laser App. 18 (2004), pp 28 - 34.

9. Thomy, C.; Vollertsen, F.: Application of Altern. Magn. Fields in Laser Welding of Aluminium. In: Proc. Of LAMP2006, 4th International Congress on Laser Advanced Materials Processing, Kyoto, Japan, 2006.

10. Gatzen, M.; Tang, Z.; Vollertsen, F.: Influence of a magnetic field in laser beam welding of aluminium. In: Proc. LAMP 2009 in Kobe/Japan, online-proceedings (http://www.jlps.gr.jp/en/proc/lamp/09/) #09-137 (#170)